Types of solutions of the variable-coefficient nonlinear Schrödinger equation with symbolic computation

Wen-Jun Liu,[1] Bo Tian,[1,2,3,*] and Hai-Qiang Zhang[1]

[1]*School of Science, Beijing University of Posts and Telecommunications, P. O. Box 122, Beijing 100876, China*

[2]*State Key Laboratory of Software Development Environment, Beijing University of Aeronautics and Astronautics, Beijing 100191, China*

[3]*Key Laboratory of Optical Communication and Lightwave Technologies, Ministry of Education, Beijing University of Posts and Telecommunications, Beijing 100876, China*

(Received 19 July 2008; published 31 December 2008)

By using Hirota's bilinear method and symbolic computation, solutions for a variable-coefficient nonlinear Schrödinger equation are obtained theoretically. It is found that the type of the solutions changes with the different choices of the group-velocity dispersion coefficient $\beta_2(z)$. According to those solutions, the relevant properties and features of physical and optical interest are illustrated. In addition, an effective technique for controlling the shape of the pulses is presented. The results of this paper will be valuable to the study of the future development of ultrahigh rate and long-distance optical communication systems.

DOI: 10.1103/PhysRevE.78.066613 PACS number(s): 05.45.Yv, 42.65.Tg

I. INTRODUCTION

In various branches of physical and engineering sciences, nonlinear evolution equations (NLEEs), especially the variable-coefficient ones, have become more and more interesting [1–3] as computerized symbolic computation rapidly develops [1–3], among which the nonlinear Schrödinger (NLS)-type models have recently riveted much attention of the researchers in long-distance optical-fiber communications [1,4–8].

In a real optical-fiber transmission system, the varying dispersion and Kerr nonlinearity are of practical importance with the consideration of the inhomogeneities resulting from such factors as the variation in the lattice parameters of the fiber media and fluctuation of the fiber's diameters [9], and the variable-coefficient NLS-type models for optical fibers are often considered to be more realistic than the standard one in that the variable coefficients can reflect the inhomogeneities of media and nonuniformities of boundaries. Therefore, investigations on the variable-coefficient NLS-type models for optical fibers have become very fruitful [4–8]. References [10,11] have demonstrated a different pulse compression technique based on exact solutions to the NLS-type equation interacting with a source, variable dispersion, variable Kerr nonlinearity, and variable gain or loss. The results of Ref. [12] have revealed that chirped soliton can all be nonlinearly compressed cleanly and efficiently in an optical fiber, which is described by the NLS equation with varying coefficients. Based on the mapping of the NLS-type equation with varying parameters to the NLS-type equation with constant dispersion and nonlinearity coefficients and an arbitrary varying gain function, Ref. [13] has presented an effective technique for finding the parabolic similariton solutions. In the case of the NLS-type equation with designed group-velocity dispersion (GVD), variable nonlinearity, and gain or loss, Ref. [14] has analytically demonstrated the phenomenon of chirp reversal crucial for pulse reproduction. Using a variable-coefficient NLS-type equation, transmission profile of a single soliton in the optical fiber with an inhomogeneous region is studied numerically in Ref. [15].

With symbolic computation [1–3], in this paper, we focus on the following variable-coefficient NLS model [16]:

$$i\left[A_z+\frac{\alpha}{2}A+\beta_1(z)A_t\right]-\frac{1}{2}\beta_2(z)A_{tt}+\gamma(z)|A|^2A=0, \quad (1)$$

where A is a complex function of z and t, the subscripts z and t denote the partial derivatives with respect to the distance and time. α is the attenuation constant, $\beta_1(z)$, $\beta_2(z)$, and $\gamma(z)$ are the inhomogeneous functions, respectively, related to the reciprocal of the group velocity, GVD, and nonlinear loss or gain. In practical applications, Eq. (1) and their various special forms [17–26] are of considerable value not only for the description of amplification or absorption and compression or broadening of optical solitons in inhomogeneous optical-fiber systems [17–21], but also for the study of stable transmission of managed solitons [18,23–26]. However, results, to the best of our knowledge, have not been seen for obtaining two or more types of solutions for Eq. (1) at one time although they are of considerable physical importance as mentioned earlier.

Being motivated by the above intriguing aspects, in the present work, we wish to undertake a detailed analysis of the dynamical features associated with the solutions for Eq. (1)

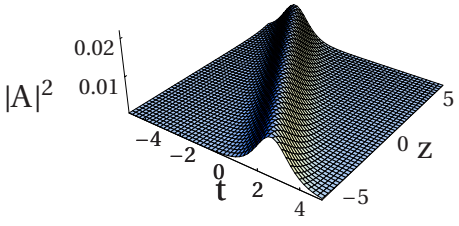

FIG. 1. (Color online) Evolution of the bright soliton via solution (12). The parameter adopted here is $\sigma=1$.

*Corresponding author: tian.bupt@yahoo.com.cn

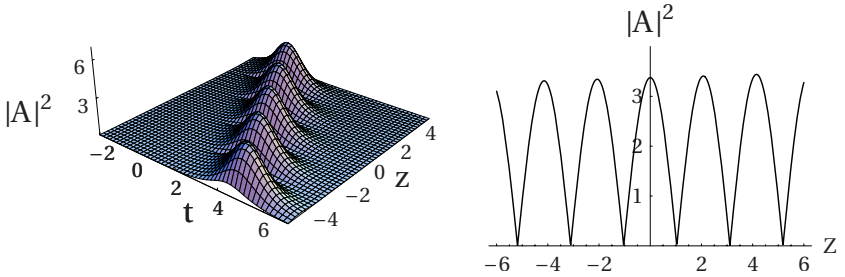

FIG. 2. (Color online) A propagating envelope pulse with the cosine profile in the DDF. The parameter adopted here is $\sigma=[\gamma(z)P_0\exp(-\alpha z)T_0^2]/|\beta_2(z)|$, $\gamma(z)=1$, $\beta_2(z)=-18\cos[\cos^{-1}(\frac{1}{18})z]$. (a) temporal evolution for the pulse, (b) the amplitude variation for the pulse at the moment of $t=0$.

to identify the various possibilities and the underlying potential technological applications. Hirota's method based on the computerized symbolic computation [1–3] has made it exercisable to solve Eq. (1). In particular, via the obtained explicit expressions for the solutions, we point out that the type of solutions depends on the coefficients of Eq. (1). To start with, we will consider the coefficients of Eq. (1) based on the dispersion profiles of the dispersion-decreasing fiber (DDF), and identify the properties of various types of solutions. Obviously, the bright soliton solutions can be found for a specific choice of soliton parameters. More interestingly, we also point out that when the coefficients are chosen as the parameters of the dispersion profiles of the DDF, there exists the periodic solutions and other solutions.

The structure of the present paper is as follows. In Sec. II, with the aid of symbolic computation, the bilinear form of Eq. (1) is obtained by use of Hirota's bilinear method. In Sec. III, some special solutions are explicitly presented based on their bilinear forms, and the detailed analysis of the solitons via the obtained soliton solutions are illustrated. Finally, our conclusions of this paper are given in Sec. IV.

II. BILINEAR FORM FOR THE VARIABLE-COEFFICIENT NLS EQUATION

In the anomalous dispersion regime $[\beta_2(z)<0]$, Eq. (1) takes the form in normalized coordinates,

$$iu_\xi+\tfrac{1}{2}u_{\tau\tau}+\sigma|u|^2u=0, \tag{2}$$

where u is the normalized amplitude and

$$\xi=\frac{\int|\beta_2(z)|dz}{T_0^2},\quad A=\sqrt{P_0}\exp\left(-\frac{\alpha}{2}z\right)u(\xi,\tau),$$

$$\tau=\frac{t-\int\beta_1(z)dz}{T_0},\quad \sigma=\frac{\gamma(z)P_0\exp(-\alpha z)T_0^2}{|\beta_2(z)|}, \tag{3}$$

in which, P_0 is the peak power of the incident pulse, τ and ξ, respectively, represent the normalized time and the normalized propagation distance. T_0 is the half-width (at $1/e$ intensity point) of the input pulse. In practice, it is customary to use the full width at half-maximum (FWHM) in place of T_0. For a hyperbolic-secant pulse, the two variables are related as $T_{\mathrm{FWHM}}=2\ln(1+\sqrt{2})T_0\approx1.763T_0$.

By introducing the dependent variable transformation [27]

$$u=\frac{g(\xi,\tau)}{f(\xi,\tau)}, \tag{4}$$

where $g(\xi,\tau)$ is a complex differentiable function and $f(\xi,\tau)$ is a real one, after some symbolic manipulations, the bilinear form of Eq. (2) is obtained as

$$\left(iD_\xi+\frac{1}{2}D_\tau^2\right)g\cdot f=0, \tag{5}$$

$$D_\tau^2 f\cdot f=2\sigma|g|^2. \tag{6}$$

Here, Hirota's bilinear operators D_ξ and D_τ [28,29] are defined by

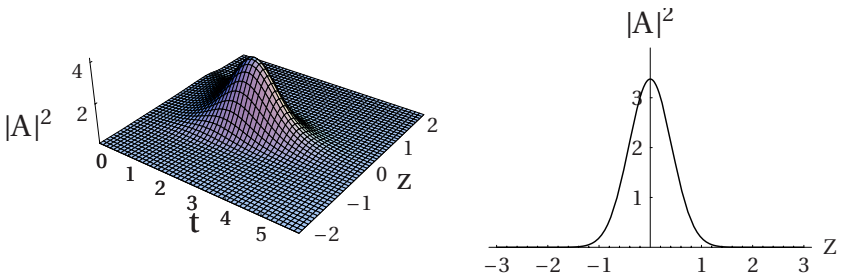

FIG. 3. (Color online) An envelope pulse with the Gaussian profile in the DDF. The parameter adopted here is $\sigma=[\gamma(z)P_0\exp(-\alpha z)T_0^2]/|\beta_2(z)|$, $\gamma(z)=1$, $\beta_2(z)=-18\exp[-(\ln 18)z^2]$. (a) Temporal evolution for the pulse, (b) the amplitude variation for the pulse at the moment of $t=0$.

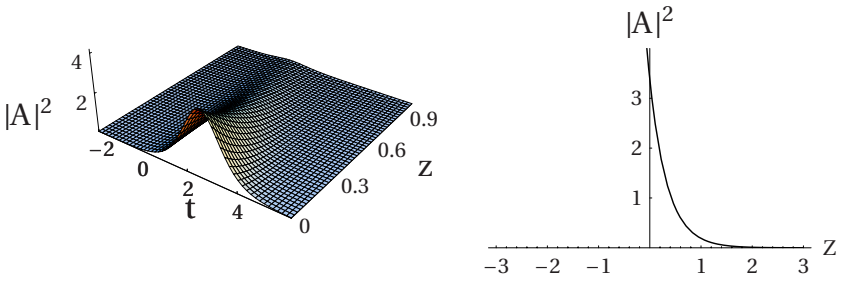

FIG. 4. (Color online) A propagating envelope pulse with the exponential profile in the DDF. The parameter adopted here is $\sigma=[\gamma(z)P_0\exp(-\alpha z)T_0^2]/|\beta_2(z)|$, $\gamma(z)=1$, $\beta_2(z)=-18\exp[-(\ln 18)z]$. (a) Temporal evolution for the pulse, (b) the amplitude variation for the pulse at the moment of $t=0$.

$$D_\xi^m D_\tau^n(a\cdot b) = \left(\frac{\partial}{\partial\xi}-\frac{\partial}{\partial\xi'}\right)^m\left(\frac{\partial}{\partial\tau}-\frac{\partial}{\partial\tau'}\right)^n a(\xi,\tau)b(\xi',\tau')\Big|_{\xi'=\xi,\tau'=\tau}. \quad (7)$$

Equations (5) and (6) can be solved by introducing the following power series expansions for g and f:

$$g=\varepsilon g_1+\varepsilon^3 g_3+\varepsilon^5 g_5+\cdots, \quad (8)$$

$$f=1+\varepsilon^2 f_2+\varepsilon^4 f_4+\varepsilon^6 f_6+\cdots, \quad (9)$$

where ε is a formal expansion parameter. Substituting Eqs. (8) and (9) into Eqs. (5) and (6) and equating coefficients of the same powers of ε to zero can yield the recursion relations for $f_n(\xi,\tau)$ $(n=2,4,6,\ldots)$ and $g_n(\xi,\tau)$ $(n=1,3,5,\ldots)$.

III. SOLUTIONS FOR THE VARIABLE-COEFFICIENT NLS EQUATION

The bilinear form for the variable-coefficient NLS equation has been presented by use of Hirota's bilinear method in Sec. II. Next, we will give some special solutions from the bilinear equations (5) and (6), exhibit the related graphics of them, and make a detailed analysis to identify the various possibilities and the underlying potential technological applications.

A. One-solitonic solution

To obtain the one-solitonic solution for Eq. (2), we assume that

$$g_1=e^{\psi}, \quad (10)$$

where $\psi=k\xi+(\eta_1+i\eta_2)\tau+\varphi_0$ with η_1, η_2, and φ_0 as arbitrary real constants, k is a pending complex parameter. Substituting g_1 into the resulting set of linear partial differential equations, and after some calculations, k is determined to be

$$k=\frac{i}{2}(\eta_1+i\eta_2)^2,$$

and

$$f_2=\frac{\sigma}{4\eta_1^2}e^{\psi+\psi^*},$$

$$g_n(\xi,\tau)=0 \quad (n=3,5,\ldots),$$

$$f_n(\xi,\tau)=0 \quad (n=4,6,\ldots), \quad (11)$$

where the asterisk denotes the complex conjugate. Without loss of generality, we set $\varepsilon=1$. Thus, the solution can be explicitly expressed as

$$u=\frac{g}{f}=\frac{g_1}{1+f_2}=\frac{e^{\psi}}{1+\dfrac{\sigma e^{\psi+\psi^*}}{4\eta_1^2}}=\frac{|\eta_1|}{\sqrt{\sigma}}e^{i\eta_2\tau+(i/2)(\eta_1^2-\eta_2^2)\xi} \times\operatorname{sech}\left[-\eta_1\eta_2\xi+\eta_1\tau+\frac{1}{2}\ln\sigma-\ln(2|\eta_1|)\right]. \quad (12)$$

According to Eq. (12), we will get different types of solutions, which are determined by the parameter σ. The value of σ mainly depends on the dispersion profile of the DDF. To

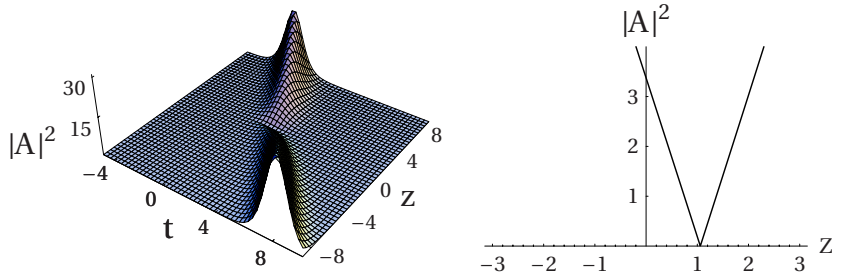

FIG. 5. (Color online) A propagating envelope pulse with the linear profile in the DDF. The parameter adopted here is $\sigma=[\gamma(z)P_0\exp(-\alpha z)T_0^2]/|\beta_2(z)|$, $\gamma(z)=1$, $\beta_2(z)=-18[1+(\frac{1}{18}-1)z]$. (a) Temporal evolution for the pulse, (b) the amplitude variation for the pulse at the moment of $t=0$.

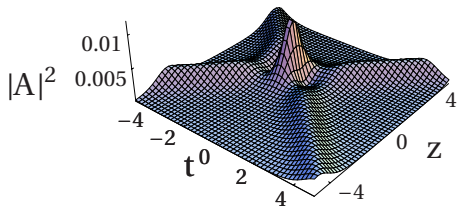

FIG. 6. (Color online) Evolution of the bright two solitons via solution (15). The parameter adopted here is $\sigma=4$.

start with, the other corresponding parameters are chosen as $\eta_1=1$, $\eta_2=-0.5$, $\varphi_0=1$, $P_0=0.01$, $T_0=4/1.732$ ps, $\alpha=4.6\times10^{-7}$ cm^{-1} ($\alpha_{\mathrm{dB}}=0.2$ dB km^{-1}), $L_{\mathrm{DDF}}=1$ km (L_{DDF} is the length of the DDF). In the following, we mainly discuss the properties of the solutions in different types.

Figure 1, with σ chosen as a constant, shows the propagation of the pulse along the distance z. The pulse is shown to propagate practically undistorted and exhibits the properties of the bright soliton which adapts to the long-distance optical-fiber transmission system. Because $\sigma=[\gamma(z)P_0\exp(-\alpha z)T_0^2]/|\beta_2(z)|$, when σ is a constant, $\gamma(z)\exp(-\alpha z)$ is proportional to $\beta_2(z)$. In this state, the effect of GVD will offset the decrease of the self-phase modulation (SPM) because of the loss, and it can be counterbalanced by the action of SPM due to the nonlinear refractive index at the same time. When $\sigma\neq$ constant, Figs. 2–5 display the different properties of Eq. (12). Here, σ is determined by the dispersion profile of the DDF.

In Fig. 2, the pulse changes along the fiber periodically when the value of $\beta_2(z)$ is chosen as the cosine profile in the DDF. The propagation direction of the pulse can also be changed by adopting the different values of η_1 and η_2. Furthermore, periodical propagation also occurs when $\beta_2(z)$ is replaced by the sine function. Thus, the phenomena of periodical changes of the pulse propagation may be due to $\beta_2(z)$, which is a periodic function in this case. In fact, at the moment of $t=0$, we can obtain from Eq. (12) that the pulse amplitude

$$|A|^2=\left[\sqrt{P_0}\exp\left(-\frac{\alpha}{2}z\right)\frac{|\eta_1|}{\sqrt{\sigma}}\right]^2=\frac{\eta_1^2|\beta_2(z)|}{T_0^2}.$$

In Fig. 2(b), $|A|^2=18\eta_1^2|\cos[\cos^{-1}(\frac{1}{18})z]|/T_0^2$ at the moment of $t=0$, so the pulse amplitude displays cyclical changes. If the cosine profile of the DDF is changed into the Gaussian profile, the corresponding pulse is obtained as shown in Fig. 3.

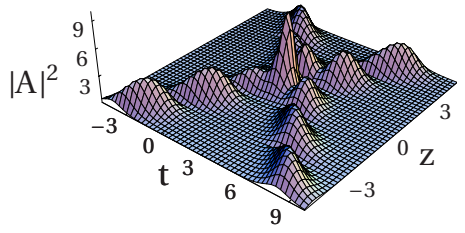

FIG. 7. (Color online) Two propagating envelope pulses with the cosine profile in the DDF. The parameter adopted here is $\sigma=[\gamma(z)P_0\exp(-\alpha z)T_0^2]/|\beta_2(z)|$, $\gamma(z)=1$, $\beta_2(z)=-18\cos[\cos^{-1}(\frac{1}{18})z]$.

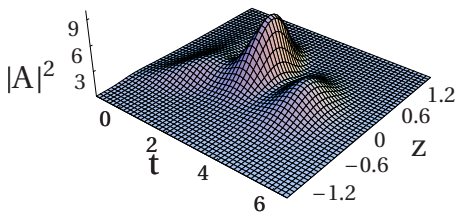

FIG. 8. (Color online) Two envelope pulses with the Gaussian profile in the DDF. The parameter adopted here is $\sigma=[\gamma(z)P_0\exp(-\alpha z)T_0^2]/|\beta_2(z)|$, $\gamma(z)=1$, $\beta_2(z)=-18\exp[-(\ln 18)z^2]$.

Figure 3 depicts a short-living pulse with the Gaussian attenuating amplitude $18\eta_1^2\exp[-(\ln 18)z^2]/T_0^2$. The pulse propagates successfully for a certain distance, but eventually it disappears due to the Gaussian profile of the DDF. The changed form of the pulse in Fig. 3(a) is further strengthened by Fig. 3(b) at the moment of $t=0$. For the exponential profile in the DDF, there exists another type of solution. Figure 4 illustrates the effect of a pulse with amplitude attenuating as it progresses along the length of the DDF. The exponentially attenuating amplitude induced by the exponential profile is $18\eta_1^2\exp[-(\ln 18)z]/T_0^2$ in this case. Correspondingly, when the dispersion profile is the linear profile, we can observe that the pulse amplitude monotonously grows during the propagation in Fig. 5. Because the pulse amplitude $|A|^2$ can be represented as $|A|^2=\eta_1^2|18-17z|/T_0^2$ at the moment of $t=0$, the pulse amplitude increases as the increase of the propagation distance. It is notable that the pulse width becomes narrow with the increase of the pulse amplitude at the same time.

B. Two-solitonic solution

The fundamental soliton cannot interact with other solitons in a single communication system under ideal conditions as discussed in Sec. III A. Whereas, there are always multiple signals in high bit rate and long-distance optical communication systems. Therefore, it is necessary to study the multisoliton transmission in a system. In this section, we mainly concentrate on the interaction between two solitons. At first, to derive the two-soliton solution, we take

$$g=g_1+g_3,\quad f=1+f_2+f_4, \tag{13}$$

where $g_1=e^{\psi_1}+e^{\psi_2}$, $\psi_j=k_j\xi+(\eta_{j1}+i\eta_{j2})\tau+\varphi_j(j=1,2)$ with η_{j1}, η_{j2}, φ_j as real constants and

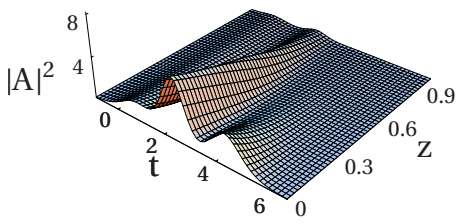

FIG. 9. (Color online) Two envelope pulses with the exponential profile in the DDF. The parameter adopted here is $\sigma=[\gamma(z)P_0\exp(-\alpha z)T_0^2]/|\beta_2(z)|$, $\gamma(z)=1$, $\beta_2(z)=-18\exp[-(\ln 18)z]$.

$$k_j = \frac{i}{2}(\eta_{j1} + i\eta_{j2})^2. \tag{14}$$

Then, by solving the resulting linear partial differential equations recursively, we can write the explicit form of the two-soliton solution as

$$u = \frac{g}{f} = \frac{g_1 + g_3}{1 + f_2 + f_4} = \frac{e^{\psi_1} + e^{\psi_2} + A_{21}e^{\psi_1+\psi_2+\psi_1^*} + A_{22}e^{\psi_1+\psi_2+\psi_2^*}}{D_1}, \tag{15}$$

where

$$D_1 = 1 + B_{21}e^{\psi_1+\psi_1^*} + B_{22}e^{\psi_2+\psi_1^*} + B_{23}e^{\psi_1+\psi_2^*} + B_{24}e^{\psi_2+\psi_2^*} + C_{21}e^{\psi_1+\psi_2+\psi_1^*+\psi_2^*},$$

with

$$A_{21} = \frac{\sigma[(\eta_{21} + i\eta_{22}) - (\eta_{11} + i\eta_{12})]^2}{4\eta_{11}^2[(\eta_{21} + i\eta_{22}) + (\eta_{11} - i\eta_{12})]^2},$$

$$A_{22} = \frac{\sigma[(\eta_{11} + i\eta_{12}) - (\eta_{21} + i\eta_{22})]^2}{4\eta_{21}^2[(\eta_{11} + i\eta_{12}) + (\eta_{21} - i\eta_{22})]^2},$$

$$B_{21} = \frac{\sigma}{4\eta_{11}^2}, \quad B_{22} = \frac{\sigma}{[(\eta_{21} + i\eta_{22}) + (\eta_{11} - i\eta_{12})]^2},$$

$$B_{23} = \frac{\sigma}{[(\eta_{11} + i\eta_{12}) + (\eta_{21} - i\eta_{22})]^2}, \quad B_{24} = \frac{\sigma}{4\eta_{21}^2},$$

$$C_{21} = \frac{\sigma^2[(\eta_{11} + i\eta_{12}) - (\eta_{21} + i\eta_{22})]^2[(\eta_{11} - i\eta_{12}) - (\eta_{21} - i\eta_{22})]^2}{16\eta_{11}^2\eta_{21}^2[(\eta_{11} + i\eta_{12}) + (\eta_{21} - i\eta_{22})]^2[(\eta_{21} + i\eta_{22}) + (\eta_{11} - i\eta_{12})]^2}.$$

In solution (15), we assume that $\eta_{11}=1$, $\eta_{12}=1$, $\eta_{21}=1$, $\eta_{22}=-1$, $\varphi_1=2$, $\varphi_2=0.5$, and observe the collision behavior between two solitons when $\beta_2(z)$ is chosen as the parameter of the dispersion profile of the DDF in Figs. 6–10.

In line with the bird's-eye view of Figs. 6–10, those analytic expressions show that solutions could be obtained by a suitable choice of the variable coefficients for each specific problem. They provide us with variable-coefficient intensity surfaces, resulted from the combined contribution of the variable coefficients in Eq. (1). Those figures imply that even if $\beta_2(z)$ is variable in different dispersion profiles, the standard elastic collisions can also occur. The pulses can interact with each other unperiodically after being input into the DDF for distances, and separate unaffected after collision. All of them vary for the function forms of $\beta_2(z)$. Therefore, illustrated in the above figures, we are able to control the shape of the pulses by managing the variable group-velocity dispersion coefficient $\beta_2(z)$ in optical soliton communication systems, which are now dispersion managed.

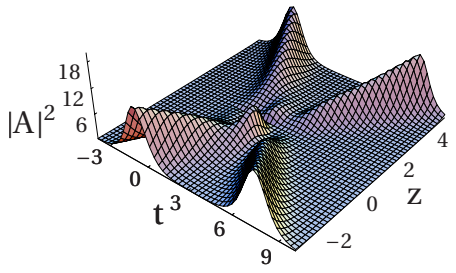

FIG. 10. (Color online) Two propagating envelope pulses with the linear profile in the DDF. The parameter adopted here is $\sigma = [\gamma(z)P_0 \exp(-\alpha z)T_0^2]/|\beta_2(z)|$, $\gamma(z)=1$, $\beta_2(z)=-18[1+(\frac{1}{18}-1)z]$.

IV. CONCLUSIONS

In this paper, we have presented an effective technique for controlling the shape of the pulses based on the variable-coefficient NLS equation, i.e., Eq. (1). Solutions for Eq. (1) have been obtained by directly applying Hirota's bilinear method. The analysis shows that the features of these solutions mainly depend on the parameter $\beta_2(z)$ describing the dispersion profiles of the DDF, and thus the pulses for shape of particles should be observed in experimental applications. The solutions allow us to characterize numerous propagation regimes useful for different applications. For instance, the soliton solution may be of certain value to the study on signal amplification and pulse compression, the periodic solution can be used in the dispersion-managed systems, and the other solutions could further effectively collect the signal envelopes or be used as the carrier in the communication systems. We anticipate that these results will have many applications in the future development of ultrahigh rate and long-distance optical communication systems.

ACKNOWLEDGMENTS

We express our sincere thanks to the referees for their valuable comments. This work has been supported by the National Natural Science Foundation of China under Grants No. 60772023 and No. 60372095, by the Key Project of Chinese Ministry of Education (Contract No. 106033), by

the Open Fund of the State Key Laboratory of Software Development Environment under Grant No. SKLSDE-07-001, Beijing University of Aeronautics and Astronautics, by the National Basic Research Program of China (973 Program) under Grant No. 2005CB321901, and by the Specialized Research Fund for the Doctoral Program of Higher Education (Contract No. 20060006024), Chinese Ministry of Education.

[1] M. P. Barnett, J. F. Capitani, J. Von Zur Gathen, and J. Gerhard, Int. J. Quantum Chem. **100**, 80 (2004); B. Tian and Y. T. Gao, Phys. Lett. A **342**, 228 (2005); **359**, 241 (2006); B. Tian, W. R. Shan, C. Y. Zhang, G. M. Wei, and Y. T. Gao, Eur. Phys. J. B **47**, 329 (2005); B. Tian, Y. T. Gao, and H. W. Zhu, Phys. Lett. A **366**, 223 (2007); W. J. Liu, B. Tian, H. Q. Zhang, L. L. Li, and Y. S. Xue, Phys. Rev. E **77**, 066605 (2008).

[2] Z. Y. Yan and H. Q. Zhang, J. Phys. A **34**, 1785 (2001); W. P. Hong, Phys. Lett. A **361**, 520 (2007); B. Tian and Y. T. Gao, *ibid.* **340**, 243 (2005); **340**, 449 (2005); Eur. Phys. J. D **33**, 59 (2005); Phys. Plasmas **12**, 054701 (2005); **12**, 070703 (2005).

[3] G. Das and J. Sarma, Phys. Plasmas **6**, 4394 (1999); Y. T. Gao and B. Tian, *ibid.* **13**, 112901 (2006); **13**, 120703 (2006); Phys. Lett. A **361**, 523 (2007); Europhys. Lett. **77**, 15001 (2007); B. Tian, G. M. Wei, C. Y. Zhang, W. R. Shan, and Y. T. Gao, Phys. Lett. A **356**, 8 (2006).

[4] E. Papaioannou, D. Frantzeskakis, and K. Hizanidis, IEEE J. Quantum Electron. **32**, 145 (1996); R. Y. Hao, L. Li, Z. H. Li, and G. S. Zhou, Phys. Rev. E **70**, 066603 (2004); R. C. Yang, L. Li, R. Y. Hao, Z. H. Li, and G. S. Zhou, *ibid.* **71**, 036616 (2005).

[5] J. Pina, B. Abueva, and G. Goedde, Opt. Commun. **176**, 397 (2000); X. H. Meng, C. Y. Zhang, J. Li, T. Xu, H. W. Zhu, and B. Tian, Z. Naturforsch., A **62**, 13 (2007).

[6] G. P. Agrawal, *Nonlinear Fiber Optics*, 3rd ed. (Academic, San Diego, CA, 2001); G. P. Agrawal, *Applications of Nonlinear Fiber Optics* (Academic, San Diego, CA, 2001); V. Serkin, M. Matsumoto, and T. Belyaeva, Opt. Commun. **196**, 159 (2001); Z. Xu, L. Li, Z. Li, and G. S. Zhou, *ibid.* **210**, 375 (2002).

[7] V. I. Karpman, J. J. Rasmussen, and A. Shagalov, Phys. Rev. E **64**, 026614 (2001); D. Mihalache, L. Torner, F. Moldoveanu, and N. -C. Panoiu, J. Phys. A **26**, L757 (1993); M. Ohta, Chaos, Solitons Fractals **4**, 2245 (1994); M. Potasek, IEEE J. Quantum Electron. **29**, 281 (1993); K. Hizanidis, D. Frantzeskakis, and C. Polymilis, J. Phys. A **29**, 7687 (1996); S. B. Medvedev, O. V. Shtyrina, S. L. Musher, and M. P. Fedoruk, Phys. Rev. E **66**, 066607 (2002); V. Marikhin, A. Shabat, M. Boiti, and F. Pempinelli, J. Exp. Theor. Phys. **90**, 553 (2000); A. Khater, M. Moussa, and S. Abdul-Aziz, Chaos, Solitons Fractals **15**, 1 (2003); A. Wingen, K. H. Spatschek, and S. B. Medvedev, Phys. Rev. E **68**, 046610 (2003); H. N. Xuan, C. J. Wang, and D. F. Zhang, Z. Naturforsch., A **59**, 196 (2004); S. Turitsyn, T. Schafer, K. Spatschek, and V. Mezentsev, Opt. Commun. **163**, 122 (1999); Y. Kubota and T. Odagaki, Phys. Rev. E **68**, 026603 (2003).

[8] K. Nakkeeran, A. Moubissi, P. Dinda, and S. Wabnitz, Opt. Lett. **26**, 1544 (2001); T. Murphy, IEEE Photonics Technol. Lett. **14**, 1424 (2002); Y. Kodama, J. Stat. Phys. **39**, 597 (1985); Y. Kodama and A. Hasegawa, IEEE J. Quantum Electron. **23**, 510 (1987); Z. Y. Yan, Chaos, Solitons Fractals **21**, 1013 (2004); A. Mahalingam and K. Porsezian, Phys. Rev. E **64**, 046608 (2001).

[9] F. Abdullaev, S. Darmanyan, and P. Khabibullaev, *Optical Solitons* (Springer-Verlag, Berlin, 1991); K. Nakkeeran, Phys. Rev. E **62**, 1313 (2000).

[10] T. S. Raju, P. K. Panigrahi, and K. Porsezian, Phys. Rev. E **72**, 046612 (2005).

[11] T. S. Raju, P. K. Panigrahi, and K. Porsezian, Phys. Rev. E **71**, 026608 (2005).

[12] R. Y. Hao, L. Li, R. C. Yang, Z. H. Li, and G. S. Zhou, Chin. Opt. Lett. **3**, 136 (2005).

[13] V. I. Kruglov and J. D. Harvey, J. Opt. Soc. Am. B **23**, 2541 (2006).

[14] R. Atre and P. K. Panigrahi, Phys. Rev. A **76**, 043838 (2007).

[15] Y. Kubota and T. Odagaki, Phys. Rev. E **68**, 026603 (2003).

[16] H. H. Kuehl, J. Opt. Soc. Am. B **5**, 709 (1988).

[17] L. Li, Z. H. Li, S. Q. Li, and G. S. Zhou, Opt. Commun. **234**, 169 (2004).

[18] S. H. Chen and L. Yi, Phys. Rev. E **71**, 016606 (2005); J. P. Tian and G. S. Zhou, Opt. Commun. **262**, 257 (2006).

[19] J. D. Moores, Opt. Lett. **21**, 555 (1996).

[20] R. Ganapathy and V. C. Kuriakose, Chaos, Solitons Fractals **15**, 99 (2003).

[21] L. Y. Wang, L. Li, Z. H. Li, G. S. Zhou, and D. Mihalache, Phys. Rev. E **72**, 036614 (2005).

[22] G. Y. Yang, R. Y. Hao, L. Li, Z. H. Li, and G. S. Zhou, Opt. Commun. **260**, 282 (2006).

[23] S. Kumar and A. Hasegawa, Opt. Lett. **22**, 372 (1997).

[24] Y. Kodama, Physica D **123**, 255 (1998); C. C. Mak, K. W. Chow, and K. Nakkeeran, J. Phys. Soc. Jpn. **74**, 1449 (2005).

[25] M. J. Ablowitz and Z. H. Musslimani, Phys. Rev. E **67**, 025601(R) (2003).

[26] V. N. Serkin and A. Hasegawa, Phys. Rev. Lett. **85**, 4502 (2000).

[27] R. Hirota, J. Math. Phys. **14**, 805 (1973).

[28] R. Hirota, Phys. Rev. Lett. **27**, 1192 (1971).

[29] J. J. Nimmo and N. C. Freeman, J. Phys. A **17**, 1415 (1984).